ISSN 0915-633X

INTERNATIONAL ATOMIC ENERGY AGENCY

THIRTEENTH INTERNATIONAL CONFERENCE ON
PLASMA PHYSICS AND CONTROLLED NUCLEAR FUSION RESEARCH

Washington, DC, United States of America, 1–6 October 1990

IAEA-CN-53/I-2-4

NATIONAL INSTITUTE FOR FUSION SCIENCE

Nonresonant Current Drive by RF Helicity Injection

A. Fukuyama, S.-I. Itoh, K. Itoh, K. Hamamatsu, V. S. Chan,
S. C. Chiu, R. L. Miller and T. Ohkawa

(Received – Oct. 16, 1990)

NIFS-59 Oct. 1990

RESEARCH REPORT
NIFS Series

NAGOYA, JAPAN

INTERNATIONAL ATOMIC ENERGY AGENCY

THIRTEENTH INTERNATIONAL CONFERENCE ON
PLASMA PHYSICS AND CONTROLLED NUCLEAR FUSION RESEARCH

Washington, DC, United States of America, 1-6 October 1990

IAEA-CN-53/ I-2-4

NONRESONANT CURRENT DRIVE BY RF HELICITY INJECTION

A. Fukuyama, S.-I. Itoh†, K. Itoh†, K. Hamamatsu††

V. S. Chan‡, S. C. Chiu‡, R. L. Miller‡, T. Ohkawa‡

Faculty of Engineering, Okayama University, Okayama 700, Japan

† National Institute for Fusion Science, Nagoya 464-01, Japan

†† Japan Atomic Energy Research Institute, Ibaraki 311-01, Japan

‡ General Atomics, P. O. Box 85608, San Diego, CA 92186-9784, U. S. A.

key words

helicity injection, current-drive, rf helicity, nonresonant force

NONRESONANT CURRENT DRIVE BY RF HELICITY INJECTION

Abstract

Current drive via nonresonant interaction between RF waves and plasma is studied by using the kinetic wave analysis and computation in a stationary state. The nonresonant interaction generates a force, in addition to the usual ponderomotive force. The force of our concern mainly acts as an internal force among plasma species; the net momentum input from the wave to the plasma is small in this process. The current driven by this process is not included in the conventional current drive scheme (i.e. resonant absorption of the parallel wave momentum or wave energy), and appears associated with the change of the RF wave helicity $\langle \widetilde{\mathbf{A}} \cdot \widetilde{\mathbf{B}} \rangle$. The analysis is applied to ICRF waves in large tokamaks. The one dimensional wave analysis code (TASK/W1) shows that the conversion ratio of the RF wave helicity to the DC helicity becomes close to one in the case of hot plasmas . The current drive efficiency by the RF helicity injection is not necessarily bounded by the conventional RF current drive efficiency. Preliminary study suggests that it scales strongly with electron temperature and toroidal magnetic field but only weakly with plasma density.

1. INTRODUCTION

One of the key issues in tokamak reactor design is the current drive efficiency. The consistency analysis on a ITER grade plasma has shown that the current drive efficiency is critical in determining circulating power, Q-value and divertor heat load [1]. A new scheme of current drive by RF wave helicity injection has been proposed [2]. If RF helicity is totally converted into DC helicity, i.e. the conversion ratio of $\lambda = \Delta \mathbf{E} \cdot \mathbf{B}_0 / \langle \widetilde{\mathbf{E}} \cdot \widetilde{\mathbf{B}} \rangle$ is unity, then a high current drive efficiency is expected. (ΔE is the reduction of DC electric field by the current drive). Extensions have been made on the MHD theory [3-5], on the mechanism of wave helicity current drive [6] and on the ICRF wave application [7]. However the relation to the conventional momentum input schemes [8] was not clear so far.

We investigate an internal force on plasma induced by RF waves. It is generated by nonresonant wave interaction in addition to the resonant force and the conservative ponderomotive force. This force is associated with source or sink of the RF wave helicity, $\langle \widetilde{\mathbf{A}} \cdot \widetilde{\mathbf{B}} \rangle$. The case of minority heating by ICRF waves is studied numerically. The conversion ratio approaches to unity in hot plasmas. It is clarified that the current drive by RF helicity injection is an independent scheme of the usual RF current drive and that the efficiency would not be bounded by the conventional limit.

2. NONRESONANT INTERNAL FORCE

The wave momentum conservation in an inhomogeneous and dispersive medium has been discussed in literatures [9-11]. We write the force **F** by the wave according to Ref. 11 as

$$\mathbf{F} = nq\left[\frac{\mathbf{k}}{\omega}\left(\widetilde{\mathbf{E}}^{*}\cdot\mathsf{M}_{\mathrm{H}}\cdot\widetilde{\mathbf{E}}\right) - \mathrm{i}\frac{\mathbf{k}}{2\omega}\frac{\partial}{\partial\mathbf{r}}\left(\widetilde{\mathbf{E}}^{*}\cdot\frac{\partial\mathsf{M}_{\mathrm{A}}}{\partial\mathbf{k}}\cdot\widetilde{\mathbf{E}}\right) + \mathrm{i}\frac{1}{2\omega}\frac{\partial}{\partial\mathbf{r}}\left(\widetilde{\mathbf{E}}^{*}\cdot\mathsf{M}_{\mathrm{A}}\cdot\widetilde{\mathbf{E}}\right) - \mathrm{i}\frac{1}{\omega}\frac{\partial}{\partial\mathbf{r}}\cdot\left(\mathsf{M}_{\mathrm{A}}\cdot\widetilde{\mathbf{E}}\,\widetilde{\mathbf{E}}^{*}\right)\right] \tag{1}$$

where n is the density, q the charge, **k** the wave number, $\omega/2\pi$ the wave frequency, M the mobility tensor and suffixes H and A stand for the Hermitian part and anti-Hermitian part, respectively. The wave is assumed to be stationary, i.e. ω is real. The first term is the force due to the wave dissipation (in the direction of **k**), the second is due to the wave dispersion (also in the direction of **k**), the third is the ponderomotive force (in the direction of the gradient) and the last is the force of present concern (in the direction of **E**). This force is due to the nonresonant interaction. The ponderomotive force is written in the form of the gradient of a potential and disappears by the flux surface average, but this nonresonant force does not. We call this force internal (polarizing) force. In the case where a single wave of $k_y = 0$ is propagating in the x-direction (z-axis is in the direction of the static magnetic field), the force in z-direction, which generates parallel current, can be written as $F_z = F_z^{\mathrm{R}} + F_z^{\mathrm{NR}}$,

$$F_z^{\mathrm{R}} = \frac{n_0 q}{\omega} k_z\, \widetilde{\mathbf{v}}^{*}\cdot\widetilde{\mathbf{E}}, \quad F_z^{\mathrm{NR}} = -\frac{n_0 q}{\omega}\left[(k_x - k_x^{*})\widetilde{v}_x^{*} + (k_z - k_z^{*})\widetilde{v}_z^{*}\right]\widetilde{\mathrm{E}}_z \tag{2}$$

where R and NR denote resonant and non-resonant, respectively. It is noted that the sum of F_z^{NR} over particle species corresponds to the change of the momentum of vacuum electromagnetic field and is usually small. This is the reason we call this force as an internal force. The RF helicity $H = \langle\widetilde{\mathbf{A}}\cdot\widetilde{\mathbf{B}}\rangle$ satisfies the conservation relation, $\dot{H} = -\nabla\cdot\mathbf{Q}_{\mathrm{H}} - 2\langle\widetilde{\mathbf{E}}\cdot\widetilde{\mathbf{B}}\rangle$, where the helicity flux $\mathbf{Q}_{\mathrm{H}}$ is defined as $\mathbf{Q}_{\mathrm{H}} = \langle\mathbf{A}\times\partial\mathbf{A}/\partial t + 2\phi\mathbf{B}\rangle$. The helicity source/sink term is given by $\langle\widetilde{\mathbf{E}}\cdot\widetilde{\mathbf{B}}\rangle$.

3 APPLICATION TO ICRF WAVES

We calculate the nonresonant force, the helicity conversion rate and the driven current. The one-dimensional slab model of a tokamak plasma is used, and the ICRF wave propagation is studied by using the TASK/W1 code [7,12]. The x-axis is taken in the direction of the major radius, and $x = 0, x = a$, and $x = b$ correspond to the magnetic axis, plasma surface and chamber radius, respectively. The fast wave antenna is placed at $x = d$ on the low field side of the torus, carrying the oscillating current in the y-direction.

Figure 1 shows the wave structure in the case of the JET plasma. Parameters are: B_T = 3.5T, $\omega/2\pi$ = 52.5MHz, D(H) plasma, $n_e(0) = 10^{20}\mathrm{m}^{-3}$, $T(0)$ = 10keV. Wave is absorbed by electron Landau damping and ion cyclotron damping. Figure 2 illustrates the spatial profile of the forces: ${F_{ez}}^{R}$ and ${F_{ez}}^{NR}$ are in (a), ${F_z}^{R}$ are in (b) and ${F_z}^{NR}$ are in (c). The driven current is in (d). The helicity flux [7] $\mathbf{Q}_H$ and the change rate of the helicity, $\langle\tilde{\mathbf{E}}\cdot\tilde{\mathbf{B}}\rangle$ are also shown in Fig.3 (a) and (b). Balancing the ${F_{ez}}^{NR}$ term with the parallel ion drag, the current induced by the nonresonant force, $\mathbf{J}^{NR}$, and $\Delta\mathbf{E}$ are calculated as

$$J_{\parallel}^{NR} = \frac{e}{m_e \nu_{ei}} F_z^{NR}, \quad \Delta E_{\parallel} = \frac{1}{ne} F_z^{NR}. \tag{3}$$

Figure 3 also shows $\Delta\mathbf{E}\cdot\mathbf{B}_0$ and $\langle\tilde{\mathbf{E}}\cdot\tilde{\mathbf{B}}\rangle$ in (c) and the conversion ratio λ in (d). The self-consistent calculation of the wave structure and forces confirms that the nonresonant force appears associated with the helicity change. The helicity conversion coefficient is close to unity near the magnetic axis. The resonant interaction of electrons with fast waves also generates current [13] as is shown in Fig. 2(d). The driven current is given by the sum of these two mechanisms.

4 SCALING STUDY

The scaling of the helicity current drive efficiency was derived previously [6] for ICRF fast wave launched from the low field side as

$$\frac{I^{NR}R}{P_{abs}} \approx 0.004 \frac{N_z T_{10}^{5/2}}{B_T^2} \tag{4}$$

valid near the ion-ion hybrid layer. Using a 1-D wave propagation code [14] which treats Landau and cyclotron damping in the WKB approximations, we study the global helicity current drive efficiency by integrating over the plasma slab. The current is calculated from helicity balance and typical density and temperature profiles are used. As an example, we chose a deuterium plasma with a hot proton minority species to achieve strong single absorption . Fig. 4(a) shows $I^{NR}R/P_{abs}$ vs. n_D. The efficiency is insensitive to density within this range as expected. We also plotted $\omega_{pi}^2/c^2k_z^2$ for the same densities. At lower densities, its value drops below unity bringing the magnetosonic cutoff close to the plasma center and the wave becomes largely evanescent. At higher densities, the mode conversion layer widens and a full wave treatment is needed to accurately calculated the absorption and current. Fig. 4(b) shows the efficiency as a function of T_e. It scales $T_e^{5/2}$ over a broad range of temperature in good agreement with Eq. (4). Note that $\omega_{pi}^2/c^2k_z^2$ is constant for this scan hence the propagation condition is held fixed. In Fig. 4(c), the efficiency is computed as B_T is varied. Since $N_z = ck_z/\omega$ and we vary ω correspondingly to keep the cyclotron resonance location fixed, Eq. (4) predicts a scaling of B_T^{-3} which fits the computed result reasonably well, with the latter showing a slightly weaker dependence. In Fig. 4(d), we vary k_z with $\omega_{pi}^2/c^2k_z^2$ held constant to avoid changing the evanescent layer. The efficiency indicates only a weak dependence on k_z which disagree with Eq. (4). Further study is needed to understand this result.

5 SUMMARY AND DISCUSSION

In this article, we identify the RF driven current by the nonresonant interaction. The total current is the sum of the two; 1)the current driven by the absorption of the RF wave momentum through resonant interaction and 2) the new current driven by the non-resonant internal (polarizing) force. The latter current appears associated with the source/sink of RF wave helicity. The case of the ICRF waves is studied. The conversion ratio λ is calculated and is found to be close to unity in large and hot plasmas. The analytic prediction of the efficiency [2,6] based on the assumption of $\lambda = 1$ has been compared with a 1-D calculation. The strong scaling with T_e and B_T and insensitivity to n_D are in agreement while the linear scaling with k_z has not been obtained.

Acknowledgements

Authors acknowledge discussions during the US-Japan workshop on "RF Helicity Current Drive" (San Diego, 1990). This work is partly supported by the Grant-in-Aid for

Scientific Research of Japanese Ministry of Education, by the contract with US Department of Energy (Contract Number DE-AC03-89ER53277) and by the collaboration program between universities and JAERI on fusion research.

References

[1] ITOH, S.-I., FUKUYAMA, A., TAKIZUKA, T., ITOH, K., Fusion Technol. **16** (1989) 346.

[2] OHKAWA, T., Comments Plasma Phys. Controlled Fusion **12** (1989) 165.

[3] BELLAN, P.M., SCHALIT, M. A., Phys. Fluids B **1** (1989) 2533.

[4] METT, R. R., TATARONIS, J. A., Phys. Rev. Lett. **63** (1989) 1380.

[5] TAYLOR, J. B., Phys. Rev. Lett. **63** (1989) 1384.

[6] CHAN, V. S., MILLER, R. L., OHKAWA, T., Phys. Fluids B **2** (1990) 944, and 1441.

[7] HAMAMATSU, K., FUKUYAMA, A., ITOH, S.-I., ITOH, K., AZUMI, M., "RF helicity injection and current drive" (NIFS Research Report, NIFS-34, 1990) submitted to Phys. Fluids B.

[8] FISCH, N. J., Rev. Mod. Phys. **59** (1987) 175.

[9] GINZBURG, V. L., The propagation of Electromagnetic Waves in Plasmas, Pergamon, Oxford (1964).

[10] MUSHA, T., Proc. IEEE **60** (1972) 1475.

[11] FUKUYAMA, A., ITOH, S.-I., ITOH, K., J. Phys. Soc. Jpn. **51** (1982) 1010.

[12] FUKUYAMA, A., NISHIYAMA, S., ITOH, K., ITOH, S.-I., Nucl. Fusion **23** (1983) 1005.

[13] KISHIMOTO, Y., HAMAMATSU, K., FUKUYAMA, A., ITOH, S.-I., ITOH, K., Nucl. Fusion **27** (1987) 549.

[14] CHIU, S. C., CHAN, V. S., HARVEY, R. W. and PORKOLAB, M., Nucl. Fusion **29** (1989) 2175.

Figure Captions

Fig. 1. The wave form on the equatorial midplane. The magnetic axis corresponds to $x = 0$ and x-axis is in the major radius direction. Fast wave antenna is located on the low low field side. Parabolic density and temperature profiles are used. Plasma parameters are chosen according to the JET plasma: $n_e(0) = 10^{20}\mathrm{m}^{-3}$, $n_e(a) = 10^{19}\mathrm{m}^{-3}$, $n_H/n_e = 5\%$, $T_e(0) =$ 10keV, $T_e(a) = 0.1$keV, $T_e = T_D = T_H$, $B(0) = 3.5$T, $\omega/2\pi = 52.5$MHz, $k_Z = 8\mathrm{m}^{-1}$ ($\omega/k_z v_{Te0}$ ≈ 0.96), and total input power is 1MW. E_x component (a), E_y component (b), E_z component (c), and power absorption profile with Poynting flux (d) are shown.

Fig. 2. Forces and driven current for the case of Fig.1. Resonant and nonresonant forces on electrons are compared in (a). Resonant forces and nonresonant forces on electrons, dueterons and protons are given in (b) and (c), respectively. The driven current is in (d): majority is driven by $\mathbf{F}_e{}^R$.

Fig. 3. Comparison with RF wave helicity for the case of Fig.1. Helicity flux (a), and helicity source/sink term (b). The change of the DC helicity $\Delta\mathbf{E}\cdot\mathbf{B}_0$ is compared to the RF helicity sink/source term in (c). The conversion ratio, $\lambda = \Delta\mathbf{E}\cdot\mathbf{B}_0 / \langle\widetilde{\mathbf{E}}\cdot\widetilde{\mathbf{B}}\rangle$, is shown in (d).

Fig. 4. Helicity current drive efficiency versus (a) density n_D, (b) electron temperature T_e, (c) toroidal magnetic field B_T, and (d) toroidal wave number k_z. For all cases, $B_T = 5$T, $\omega = \omega_{cD0}$, $T_{e0} = T_{D0} = 10$keV, $T_{H0} = 80$keV, $n_H/n_D = 0.1$, and $k_z = 25\mathrm{m}^{-1}$, unless specified otherwise.

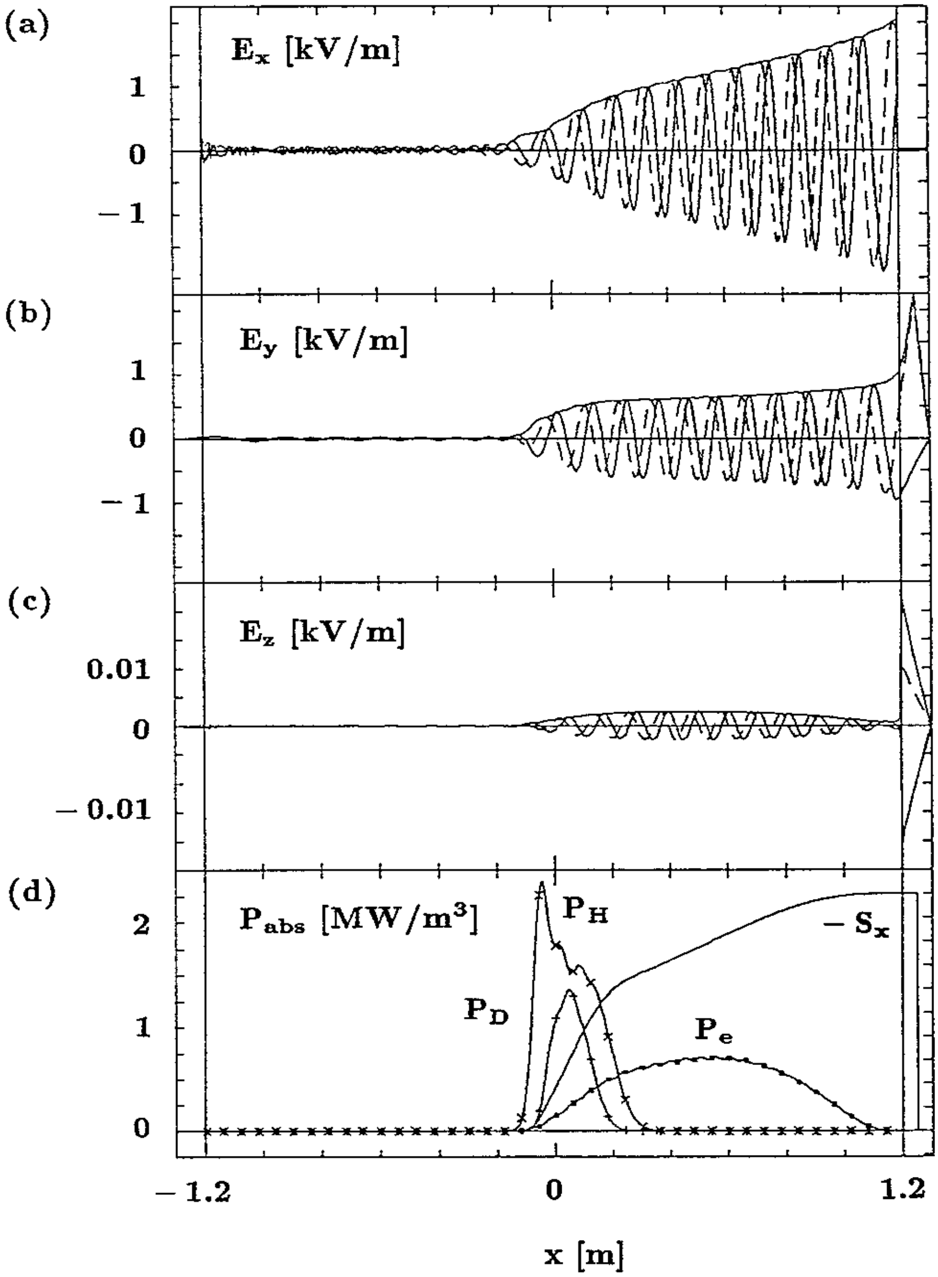

(a)
Ex [kV/m]
1
0
− 1
(b)
Ey [kV/m]
1
0
− 1
(c)
Ez [kV/m]
0.01
0
− 0.01
(d)
Pabs [MW/m³]
PH
− Sx
PD
Pe
2
1
0
− 1.2
0
1.2
x [m]

Fig. 1

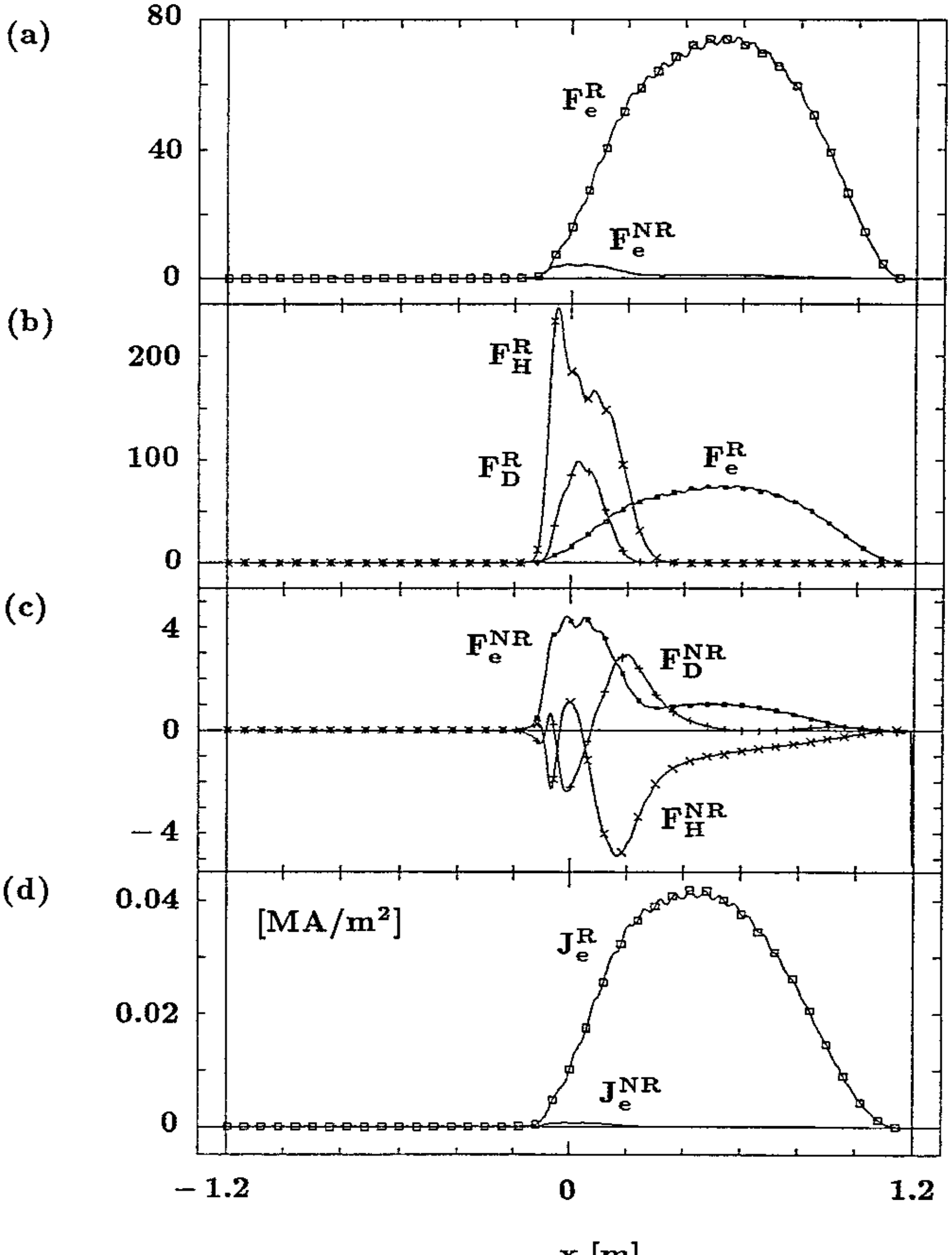

(a)
80
40
0
F_e^R
F_e^{NR}
(b)
200
100
0
F_H^R
F_D^R
F_e^R
(c)
4
0
−4
F_e^{NR}
F_D^{NR}
F_H^{NR}
(d)
0.04
0.02
0
[MA/m²]
J_e^R
J_e^{NR}
−1.2
0
1.2
x [m]

Fig. 2

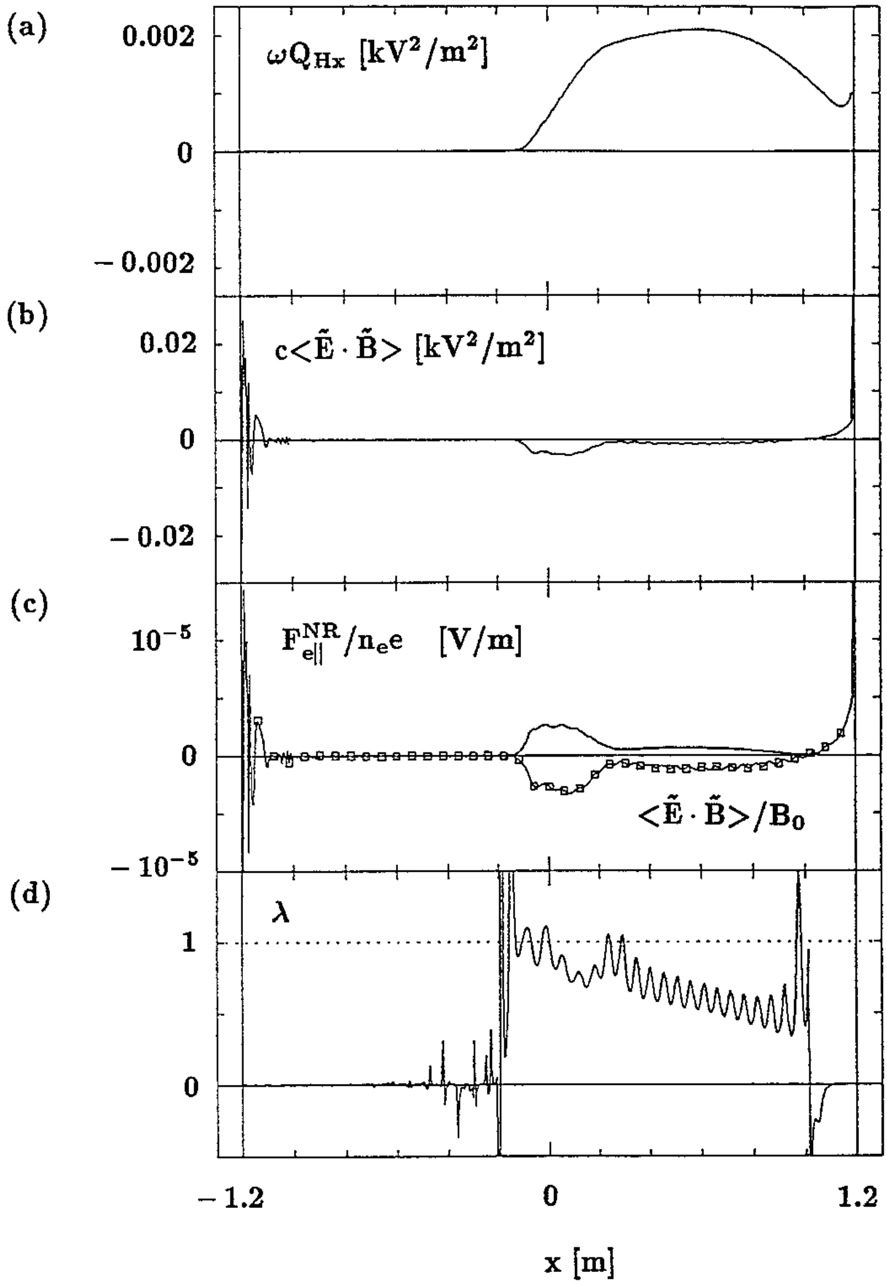

(a)
0.002
ωQ_Hx [kV²/m²]
0
− 0.002
(b)
0.02
c<Ẽ · B̃> [kV²/m²]
0
− 0.02
(c)
10⁻⁵
F_e||^NR/n_e e [V/m]
0
<Ẽ · B̃>/B₀
− 10⁻⁵
(d)
λ
1
0
− 1.2
0
1.2
x [m]

Fig. 3

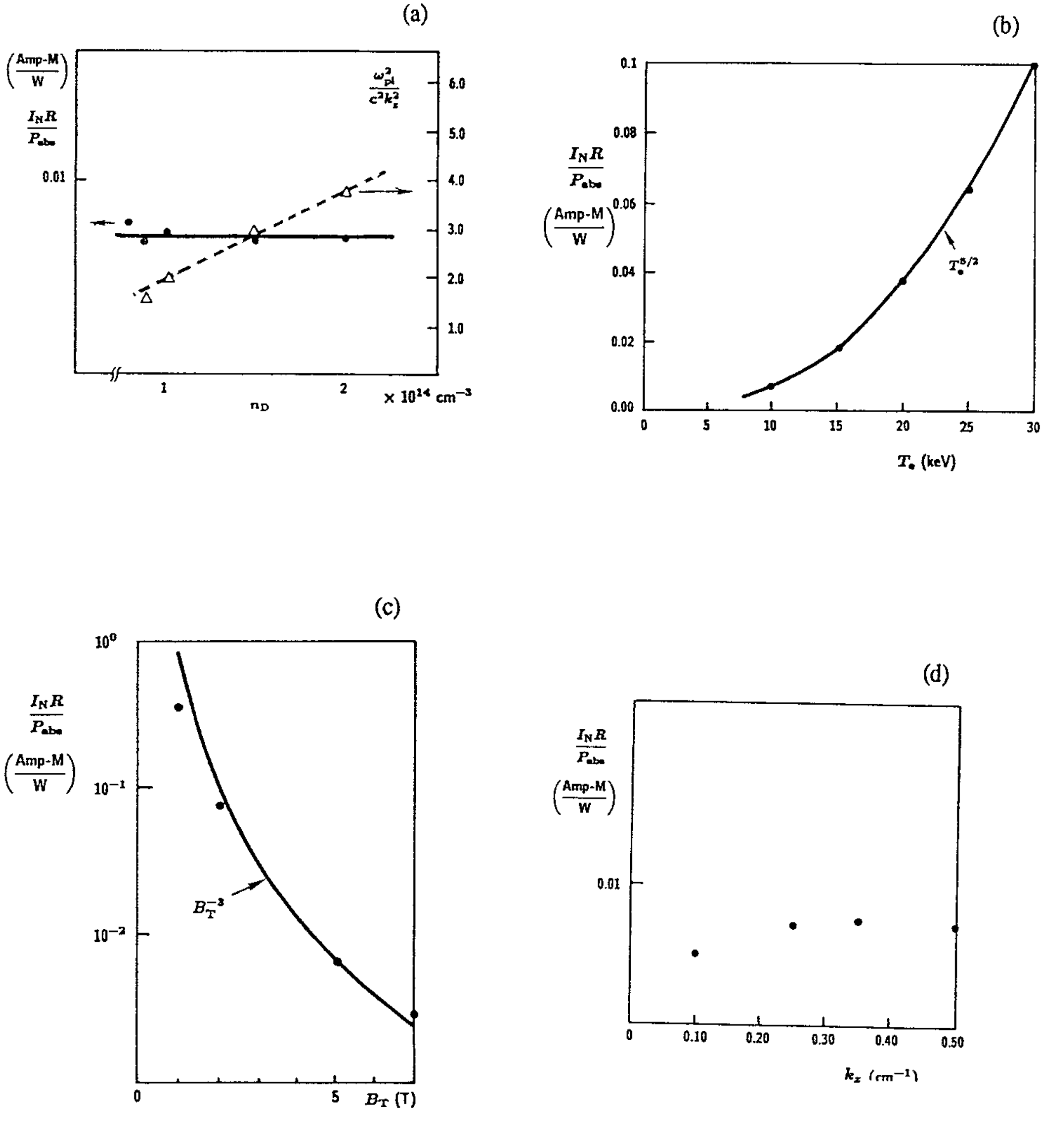

(a)
$\left(\frac{\text{Amp-M}}{\text{W}}\right)$
$\frac{I_N R}{P_{abs}}$
0.01
$\frac{\omega_{pi}^2}{c^2 k_z^2}$
6.0
5.0
4.0
3.0
2.0
1.0
1
2
$\times 10^{14}$ cm^{-3}
n_D
(b)
0.1
0.08
$\frac{I_N R}{P_{abs}}$
$\left(\frac{\text{Amp-M}}{\text{W}}\right)$
0.06
0.04
0.02
0.00
$T_e^{5/2}$
0
5
10
15
20
25
30
T_e (keV)
(c)
10^0
$\frac{I_N R}{P_{abs}}$
$\left(\frac{\text{Amp-M}}{\text{W}}\right)$
10^{-1}
B_T^{-3}
10^{-2}
0
5
B_T (T)
(d)
$\frac{I_N R}{P_{abs}}$
$\left(\frac{\text{Amp-M}}{\text{W}}\right)$
0.01
0
0.10
0.20
0.30
0.40
0.50
k_z (cm^{-1})

Fig. 4